Analysis of Electrical Load Characteristics of HX_D1B locomotive based on measured data

Wu Liran, Wu Mingli, Song Kejian
School of Electrical Engineering, Beijing Jiaotong University Beijing, China
Email: cggd2012@126.com, mlwu@bjtu.edu.cn, songkejian1988@163.com

***Abstract*-This paper firstly introduces the main circuit of traction drive system of HX_D1B locomotive, and gives the operating principle of a single phase four-quadrant PWM rectifier. Then based on measured data, the power factor and harmonics characteristics of HX_D1B are analyzed. The statistical rules on the power factor and harmonic contents are summarized, which can be used to build a probabilistic model for the HX_D1B locomotive.**

I. INTRODUCTION

With the development of power electronics technology, AC drive locomotives are widely used in traction applications. The pulse width modulation (PWM) rectifiers, with less distortion of the input current waveform, unity power factor, and bi-directional power flow, have substituted phase-controlled rectifiers in AC electric railway locomotives [1]. However the input current harmonics still exist [2] and have a broader spectrum then that of conventional DC drive locomotives. Some high order harmonics can even cause the resonance phenomenon in traction networks. So the high order harmonics characteristics of AC drive locomotives must be understood well.

At present, some methods, such as the switching function and the duty cycle, are used in modeling to simulate the current harmonics behaviours [3][4]. However, the control strategy and parameters of the control system are generally not public. Affected by the railway line condition and the operation of the train driver, the current harmonics characteristics of a locomotive are irregular [5]. Thus, the modeling methods based on the analysis of main circuit and control system are difficult to describe accurately the harmonics characteristics of a locomotive on the actual railway line. This paper, using a large quantity of measured data, takes HX_D1B locomotive as an example to analyze the harmonics characteristics when the locomotive running on the actual railway line.

II. HX_D1B LOCOMOTIVE

The axle-type of HX_D1B locomotive is Co-Co, with two bogies and six axles totally. The rated power of AC traction motor is 1600 kW per axle, and the total tractive power is 9600 kW.

A. Structure of traction drive system

The main circuit of HX_D1B locomotive consists of a main transformer, two traction converter systems and six induction motors. The secondary side of the main transformer has four traction windings. As shown in Fig.1, every two traction windings, as a group, are connected to an AC-DC-AC converter system. Each AC-DC-AC converter system consists of a dual-cascading four-quadrant rectifier, a DC link, which is shared by the two rectifiers, and three PWM three-phase inverters. Every inverter drives an asynchronous motor.

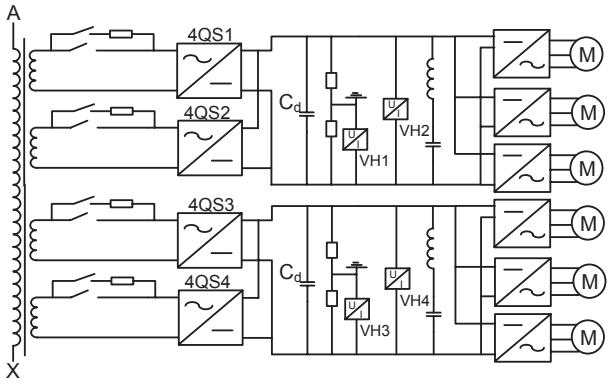

Fig.1 Traction drive system of HX_D1B locomotive

B. Single phase four-quadrant PWM rectifier

The circuit of a single phase PWM four-quadrant rectifier is shown in Fig.2, where u_s is the AC source voltage, L_s is transformer's equivalent leakage inductance, R_s is the equivalent resistance, u_{ab} is the input voltage of the rectifier, C_d is the DC link capacitor, and R_L is the equivalent DC load. Through making the power switching devices turned on and shut off reasonably, the input voltage and current can be adjusted so that the current can track the AC source voltage and achieve unity power factor.

A simple equivalent circuit of the single phase PWM rectifier on AC side has been shown in Fig.3. The voltage balance equation of the single phase PWM rectifier can be written as

$$u_s(t) = u_{ab}(t) + L_s \frac{di_s(t)}{dt} + R_s i_s(t) \tag{1}$$

In general, because the equivalent resistance on AC side is very small, it can be ignored. From (1), the input current of single phase PWM rectifier i_s can be written as

$$i_s = i_s(t_0) + \frac{1}{L_s}\int [u_s(t) - u_{ab}(t)]dt \tag{2}$$

where $i_s(t_0)$ is the initial value.

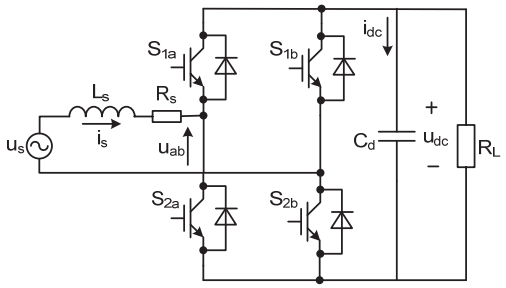

Fig.2 Topology of single phase PWM rectifier

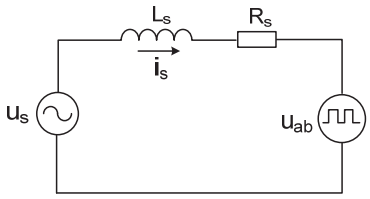

Fig.3 Equivalent circuit of single phase PWM rectifier

C. *AC current harmonics*

The realization methods of PWM can be divided into the single-polarity PWM and the dual-polarity PWM as shown in Fig.4. Intersections of carriers (the triangular waves) and the modulation wave (the sinusoidal wave) determine the turning on and shutting off of the two power switching devices in a leg. The AC input voltage of a single phase PWM rectifier u_{ab} is a series of pulses with an amplitude of U_{dc} or $-U_{dc}$.

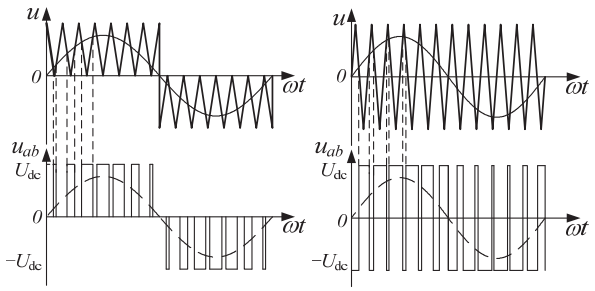

(a) single-polarity PWM (b) dual-polarity PWM

Fig.4 Schematic diagram of PWM modulation

Equation (2) shows that the input current of a single phase rectifier depends on the input voltage u_{ab} and the AC power voltage u_s. In both kinds of PWM methods, u_{ab} has a lot of harmonic components. In general, the single-polarity PWM has better harmonics characteristics than the dual-polarity PWM. Taking it as an example, we can describe u_{ab} as (3) [6] using the double Fourier transform algorithm.

$$u_{ab} = MU_{dc}\sin(\omega t-\phi)+\frac{2U_{dc}}{\sigma}\sum_{m=1,2,3\cdots}^{\infty}\sum_{n=\pm1,3,5\cdots}^{\infty}\frac{J_n(mM\sigma)}{m}\cos(m\sigma)\sin[(m(2N)+n)\omega t-n\phi)] \quad (3)$$

where M is the modulation index, N is the frequency modulation ratio, ϕ is the initial carrier phase angle, f_c is the carrier frequency, $\sigma=\pi f_c$, J_n is n order Bessel function. Equation (3) shows that u_{ab} contains certain harmonics and the harmonics are inherent in PWM. The AC power voltage can be written as

$$u_s = \sqrt{2}U_s\sin(\omega t) \quad (4)$$

From (2) to (4) we can conclude that the input current i_s has the same harmonic components as the input voltage u_{ab}. The value of harmonic components depends on the modulation method and circuit parameters.

III. ANALYSIS OF MEASURED DATA

On December 9th, 2013, a tested HX_D1B locomotive in a freight train service took a round-trip between Xiangtang and Jiujiang West in Beijing-Jiujiang electric railway. The AC voltage and current of the HX_D1B locomotive were measured. According to the measured data, the active power (P), reactive power (Q) and power factor (PF) of the HX_D1B locomotive were calculated. Fig.5 shows the active power, reactive power, and power factor from 20:00 to 21:00. The black line is P, red line is Q and blue line is PF. The value of active power and power factor can reflect the working conditions of the locomotive: traction condition when $P>0$; regenerative braking condition when $P<0$; idle running when $P\approx0$. So the measured currents can be used to analyze the harmonics characteristics of the HX_D1B locomotive in different working conditions.

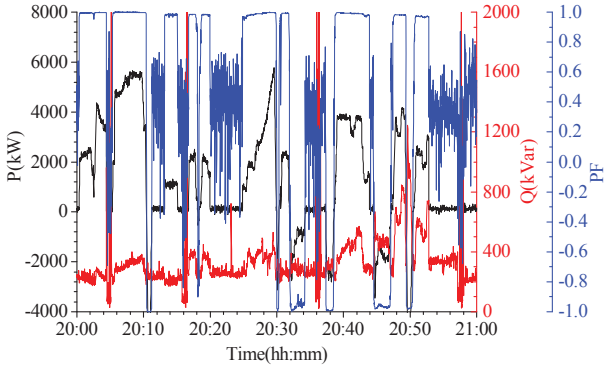

Fig.5 Active power(P), reactive power(Q) and power factor(PF)

A. *Characteristics of power factor*

Fig.6 shows the scatter diagram and fitting curve of the power factor. The maximum active power is about 8000kW in traction condition and -7000kW in regenerative braking condition. In traction condition, the power factor approaches 0.97 when the active power reaches 1000kW. With the active power increasing, the power factor becomes close to 1 rapidly; in regenerative braking condition, the power factor approaches -0.85 when the active power reaches -500kW. With active power increasing, the power factor becomes close to -1 rapidly.

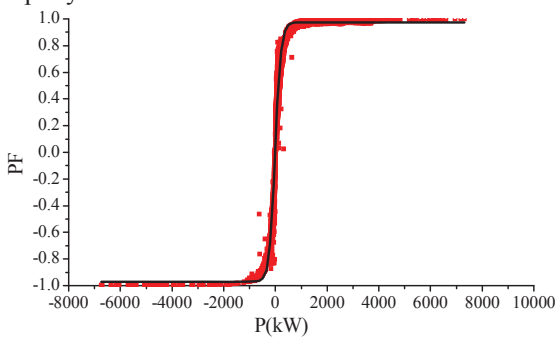

Fig.6 Scatter diagram and fitting curve of power factor

The absolute value of power factor |*PF*| in different conditions can reflect the features of power factor in large active power as shown in Fig. 7. It shows that:

1) |*PF*| > 0.96, when |*P*| > 1700kW;

2) |*PF*| > 0.996, when |*P*| > 4000kW.

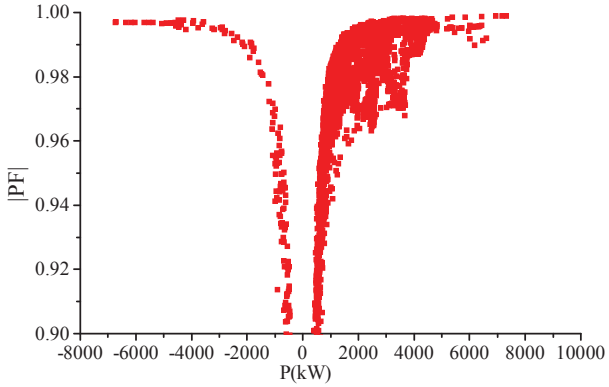

Fig.7 Scatter diagram of the absolute value of power factor

The black line in Fig. 6 is the fitting curve of power factor using Boltzmann function. The expression of the fitting curve is

$$PF = 0.975 + \frac{-0.96 - 0.975}{1 + e^{\frac{P+10.3}{110.8}}} \quad (5)$$

where *P* is active power, kW.

B. Analysis of main current harmonics

The main current harmonics can be divided into two parts: the low-order harmonics and the high-order harmonics. The measured data can clearly explain the low and high order current harmonics characteristics.

Fig.8(a) gives the voltage and current waveforms in a typical traction condition and Fig.8(b) in a typical regenerative braking condition. The black line is the voltage and the red line the current.

As shown in Fig.8, the traction current and the regenerative braking current have the same harmonic components: in low-order harmonics, the content of 3rd harmonic is greater than others; in high-order harmonics, the contents of odd order harmonics from 53rd to 79th are greater than others. Table I shows the values of main harmonic contents in both traction condition and regenerative braking condition.

As shown in Table I, the contents of odd order harmonics from 53rd to 79th are much lower than that of 3rd harmonic. In order to analyze the total influence of the main odd order harmonics, $I_{H\_53rd\sim79st}$ is calculated as shown in (6).

$$I_{H\_53rd\sim79st} = \sqrt{\sum_{i=53,57,\cdots,79} I_{hi}^{\,2}} \quad (6)$$

Fig.9 shows the fundamental current (I_{1st}), 3rd harmonic current (I_{H_3rd}), and $I_{H\_53rd\sim79st}$ when the HX_D1B locomotive was in traction condition or regenerative braking condition (I_{1st} > 13A). I_{H_3rd} varies between 3 and 12A, $I_{H\_53rd\sim79st}$ varies between 1 and 8A.

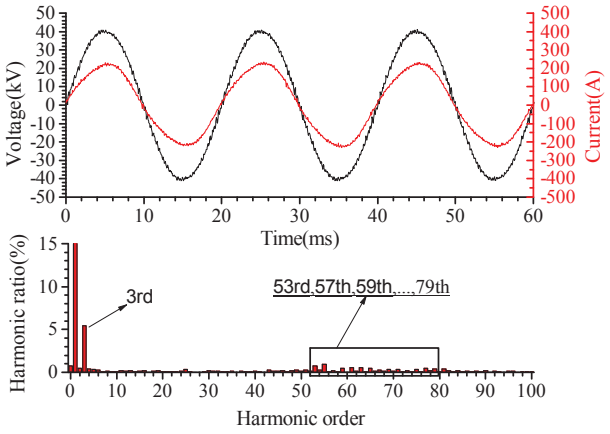

(a) traction condition

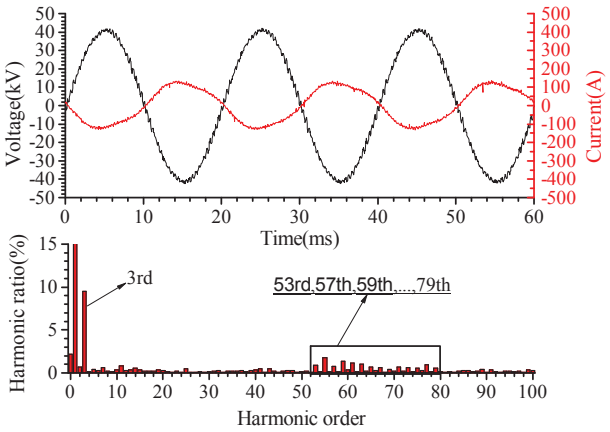

(b) regenerative braking condition

Fig.8 Voltage, current and harmonic spectrum of the current

TABLE I

MAIN HARMONIC CONTENT OF THE INPUT CURRENT

Fundamental or harmonic order	RMS(A)		Harmonic ratio(%)	
	Traction	Regenerative Braking	Traction	Regenerative Braking
1	155.22	87.86	100	100
3	8.39	8.33	5.41	9.48
53	1.12	0.80	0.72	0.91
55	1.45	1.57	0.93	1.78
57	0.31	0.64	0.20	0.73
59	0.74	1.22	0.48	1.38
61	0.81	1.00	0.52	1.14
63	0.88	0.91	0.56	1.04
65	0.77	0.59	0.49	0.67
67	0.41	0.51	0.26	0.58
69	0.53	0.38	0.34	0.43
71	0.55	0.62	0.35	0.71
73	0.34	0.53	0.22	0.60
75	0.58	0.48	0.37	0.55
77	0.74	0.81	0.47	0.92
79	0.64	0.47	0.41	0.54

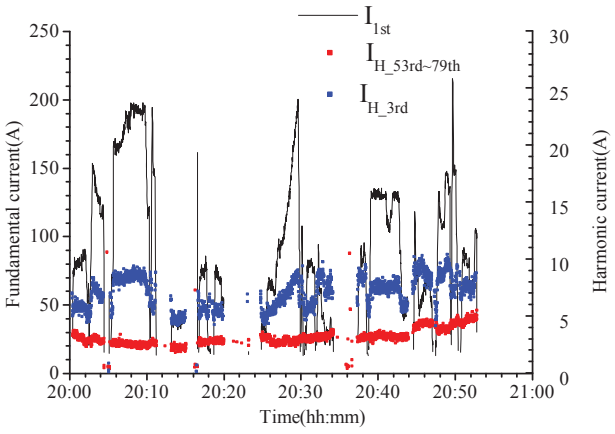

Fig.9 I_{1st} , I_{H_3rd}, $I_{H\_53rd\sim79st}$

There are different harmonics characteristics in different ranges of the active power. Fig.10 gives the total harmonic current (I_H), I_{H_3rd} and $I_{H\_53rd\sim79st}$ in different ranges of the active power.

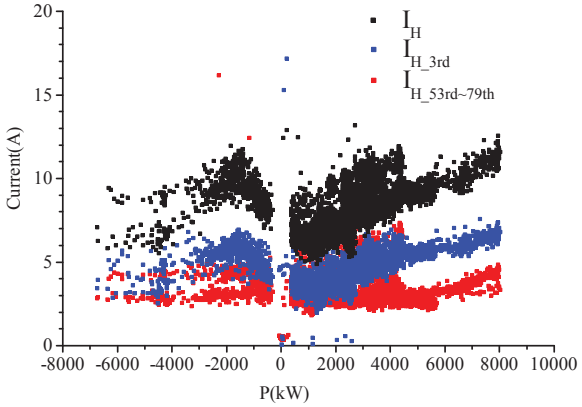

Fig.10 Scatter diagram of I_{1st} , I_{H_3rd} and $I_{H\_53rd\sim79st}$

Taking the 3rd and 55th harmonic currents as examples, the scatter diagram of current harmonic ratio and the fitting curves are gave to analyze the relationship between current harmonic ratio and fundamental current as shown in Fig.11, 12 and (7), (8).

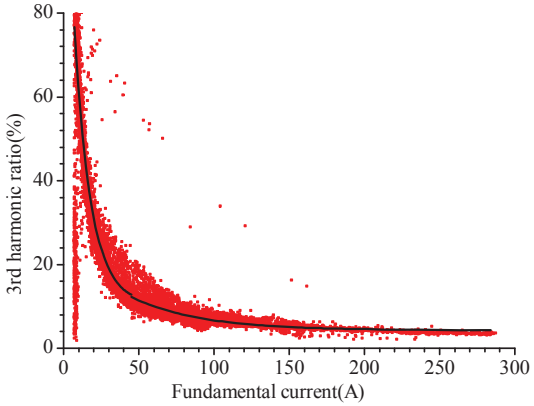

Fig.11 Scatter diagram and fitting curve of 3rd current harmonic ratio - fundamental current

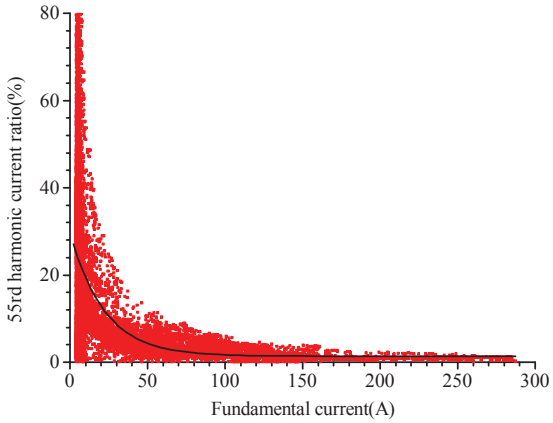

Fig.12 Scatter diagram and fitting curve of 55th current harmonic ratio - fundamental current

$$I_{3rd}(\%) = \begin{cases} 10.6 + 123.75e^{-I/11.15} & \text{when } I < 45 \\ 4.28 + 21.2e^{-I/45.88} & \text{when } I > 45 \end{cases} \quad (7)$$

$$I_{55th}(\%) = 1.39 + 28.29e^{-I/22.16} \quad (8)$$

where I is fundamental current, A.

In order to analyze the relationship between total high-order harmonic current ratio and fundamental current, scatter diagram of $I_{H\_53rd\sim79st}$ - fundamental current and its fitting curve are shown in Fig.13 and (9).

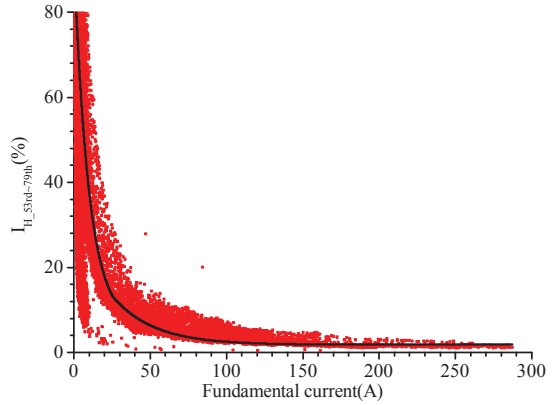

Fig.13 Scatter diagram and fitting curve of $I_{H\_53rd\sim79st}$ (%) - fundamental current

$$I_{H\_53rd\sim79th}(\%) = \begin{cases} 6.75 + 85.66e^{-I/9.84} & \text{when } I < 25.7 \\ 2.82 + 29.2e^{-I/26.9} & \text{when } I > 25.7 \end{cases} \quad (9)$$

where I is fundamental current, A.

The above content is all about the value of current harmonics, taking the 3rd harmonic current as an example, some statistical rules about current harmonic phase will be analyzed.

Fig.14 is the scatter diagram of the 3rd harmonic current in polar coordinates taking the phase of fundamental current as a reference. The polar radius of the scatters presents value of the 3rd harmonic current and the polar angle the 3rd harmonic current phase.

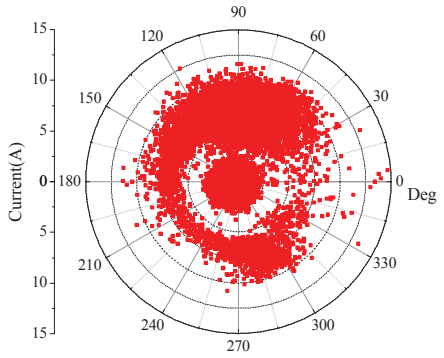

Fig.14 Scatter diagram of 3rd harmonic current in polar coordinates

Scatters can be divided into four parts as shown in Fig.14. It can be seen that scatters are distributed in the four quadrants evenly when the polar radius r < 3.5 A; scatters are mainly distributed in the first and second quadrants from 30° to 150° when 3.5 A < r <5.5A; scatters are distributed in the four quadrants evenly when 5.5 A < r < 12A; the polar angles are close to 0 when r > 12 A.

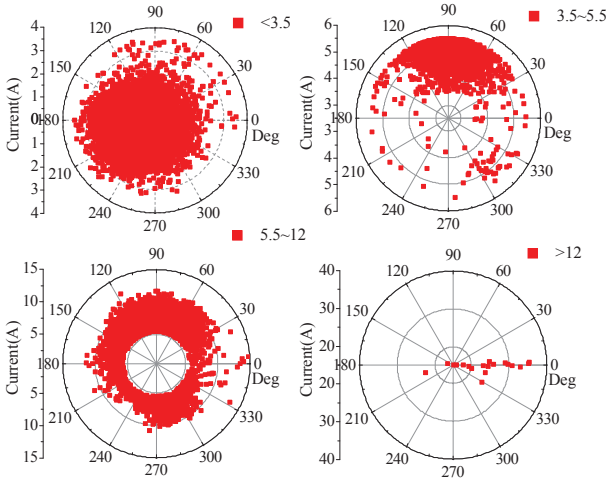

Fig.15 Scatter diagram of 3rd harmonic current

The working condition and fundamental current are two principal factors of the 3rd harmonic current phase. Fig.16 gives scatter diagram of the 3rd harmonic current phase.

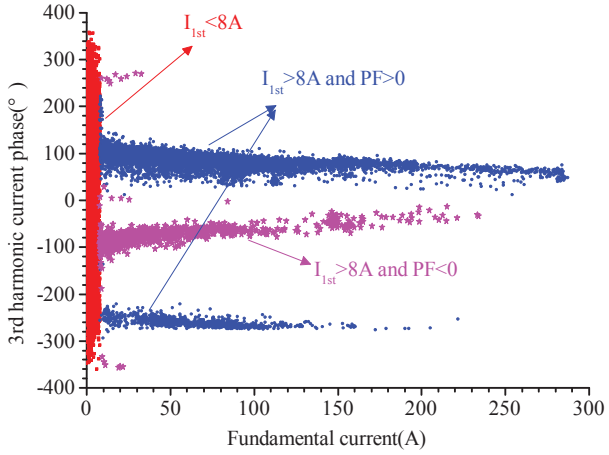

Fig.16 Scatter diagram of 3rd harmonic current phase

As shown in Fig.16, it can be seen that:

1) Scatters are distributed in -360° ~ 360° evenly when I_{1st} < 8A;

2) Most scatters are distributed in 20° ~ 100° and a small part around -245° when I_{1st} > 8A and PF > 0. The phase decreases when fundamental current increases;

3) Scatters are distributed in -100° ~ 0° when I_{1st} > 8A and PF < 0. The phase becomes close to 0gradually when fundamental current increases.

C. Current THD

Fig.17 and 18 give scatter diagrams of the current total harmonic distortion (THD_i) and fitting curves in different active power or fundamental current.

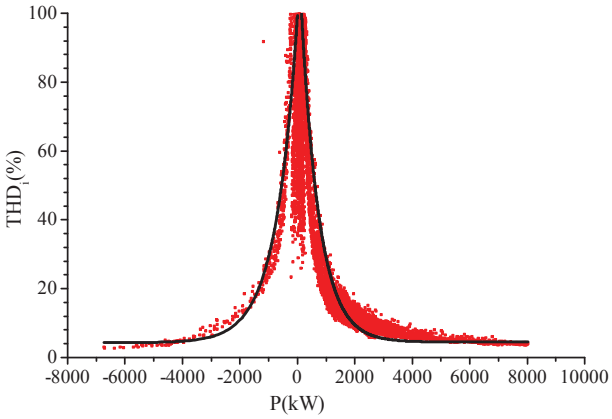

Fig.17 Scatter diagram and fitting curve of THD_i - active power

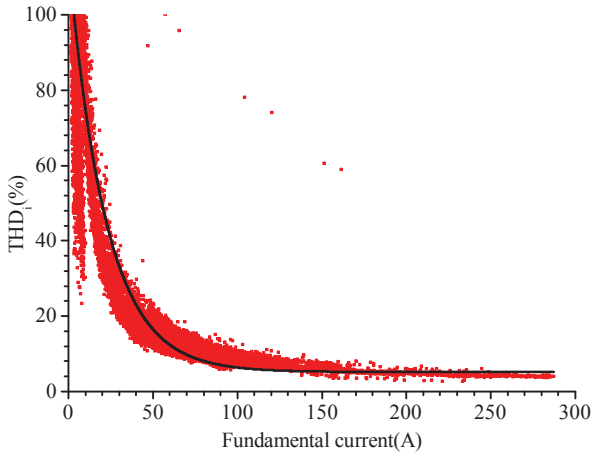

Fig.18 Scatter diagram and fitting curve of THD_i- fundamental current

As shown in Fig.17, scatters fluctuate wildly when the locomotive is idle running; THD_i decreases and tends to a small fixed value when $|P|$ increases in traction and regenerative braking conditions. The fitting curve is shown in (9). Scatter diagram in Fig.18 is similar to that in Fig.17 when P > 0. The fitting curve is shown in (10).

$$THD_i(\%) = \begin{cases} (4.3 + 95e^{P/750}) \text{ when } P < 0 \\ (4.5 + 120e^{-P/630}) \text{ when } P > 0 \end{cases} \quad (9)$$

$$THD_i(\%) = 5.2 + 110e^{I/22} \quad (10)$$

where P is active power, kW. I is fundamental current, A.

IV. CONCLUSION

This paper introduces the main circuit of traction drive system of HX_D1B locomotive, then based on measured data, analyzes the power factor, harmonics characteristics, and provides fitting functions of the power factor and total harmonic distortion. It can be summarized as follows:

In traction condition, the power factor of HX_D1B locomotive approaches 0.97 when active power reaches 1000kW. With active power increasing, the power factor becomes close to 1 rapidly; in regenerative braking condition, the power factor approaches -0.85 when active power reaches -500kW. With active power increasing, the power factor becomes close to -1 rapidly.

The 3rd harmonic is the main low-order current harmonic and the odd order harmonics from the 53rd to 79th are main high-order current harmonics. Scatters of the 3rd harmonic are distributed in four quadrants of polar coordinates. In different working conditions and fundamental currents, the 3rd harmonic current phases vary according to some rules.

The relationship between power factor and active power of HX_D1B locomotive meets the Bessel function. The relationship between the current THD and active power meets the natural exponential function.

The statistical rules on the power factor and current harmonic contents in this paper can lay a foundation for the probabilistic model of the HX_D1B locomotive.

ACKNOWLEDGMENT

The authors wish to acknowledge the financial supports from the Fundamental Research Funds for the Central Universities (under grant 2012JBZ006) and the Railway Company Science and Technology Development Planning (under grant 2014J009-B).

REFERENCES

[1] Flinders, F., and W. Oghanna. “Energy efficiency improvements to electric locomotives using PWM rectifier technology,” (1995): 106-110.

[2] O. Stihi, and B.T. Ooi, “A single-phase controlled-current PWM rectifier,” *IEEE Transactions on Power Electronics*, 3(4):453-459, 1988.

[3] Zhang Xing, Zhang Chongwei. *PWM rectifier and its control*. CA: Beijing, 2012, pp.49-65.

[4] Feng Xiaoyun. *Electric traction AC drive and control system*, CA: Chengdu,2009, pp.79-84.

[5] Tian Yusheng, Jiang Qirong, Tian Xu. “The study of the electric locomotive harmonic model based on the probability of harmonic current source,” *Advanced Technology of Electrical Engineering and Energy*. 2012, 31(3):11-15.

[6] Zhang Zhixue. “The harmonic analysis of single-phase voltage source PWM converter,” *Converter Technology & Electric Traction*. 5, 17-22,2006.